Building simulation model of an artificial egg incubator during preheat time

L. G. Rakotoarimanana[1]*, Z. A. Randriamanantany[2], F. Garde[3], T. A. Mara[3]

[1] Laboratoire de Mécanique et Physique de l'Environnement, Faculté des Sciences d'Antananarivo
[2] Laboratoire de Thermodynamique, Thermique et Combustion, Faculté des Sciences d'Antananarivo,
[3] Laboratoire de Physique du Bâtiment et des Systèmes, Université de la Réunion,

_____
* Corresponding author, e-mail: graffinliva@hotmail.com

Abstract

The aim of the present study is to build simulation model able to predict temperature and vapor concentration distributions in the artificial incubator during preheat time in order to optimize system functioning. Discretizing methods as well as simplifying hypotheses are applied to mass and heat transfer analysis which are derived from physical phenomena. These equations written in matrix form can determine physical parameters of the incubator during preheat time. Comparison between model results and measurements has been carried out. Results are in good agreement with those obtained in the experimentation in steady state. This paper proposes a simulation model and validation elements of an artificial egg incubator.

Keywords: Simulation, model, egg incubator, preheat, vapor, hatching

1. INTRODUCTION

The study of the biological room tied to the field of food processing, including the incubator, has been, among other things, one of the themes of thermal studies. Recently, research undertaken in the field of incubators has intended to enhance the rate of hatching eggs by determining the physical factors. Whereas most of the thermal studies apply to the building, we worked out a mathematical model of the incubator. This mathematical model must be able to predict primarily the vapor concentration and the temperature inside the enclosure during preheats time as well as the time of equilibrium. The space inside the incubator is subdivided into several zones. The mass and thermal balances for all zones are written in matrix form and were solved under Matlab®.

In this paper, section 2 develops the system's description and modelling methodology in which mass and heat balance are established. Section 3 presents the model results and compares them to the experiment measure.

2. SYSTEM DESCRIPTION AND MODELLING METHODOLOGY

2. 1. The incubator and its characteristics

The system is an incubator of 70 dm^3 volume, 40 eggs capacity, using 200 Watts of an electric output power. This system is conceptualised according to Wageiningen's building techniques of an artificial incubator [1] and is similar to the Yatter's model [2]. The dimensions of the incubator are given in table 1.

Table 1: Internal and external dimensions of the incubator.

Dimensions	*Length (m)*	*Width (m)*	*Height (m)*
External	0.58	0.38	0.40
Internal	0.52	0.32	0.20

The incubator has a ventilation device, a heating device and a humidifying component as shown in figure 1. Its insulating walls are composed by polystyrene squeezed between two woods.

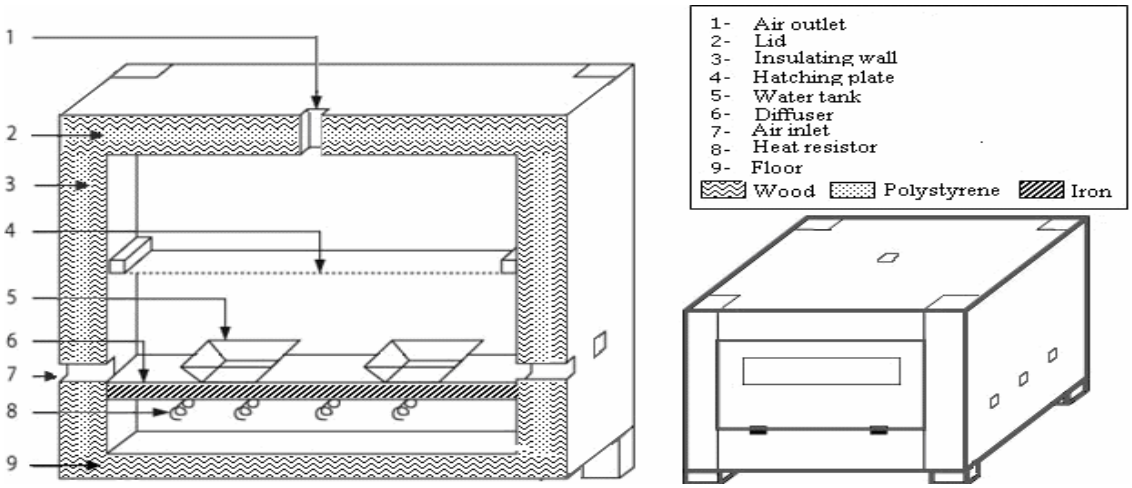

Figure 1: Diagram and transverse section of the incubator

2. 2. Hypotheses

The system has several complex physical phenomena. The following simplifying hypotheses were adopted in the heat and mass transfer balances.

- The external temperature, humidity and pressure are constant.
- The pressure of the humid air inside the incubator is equal to the atmospheric pressure. This air behaves like a perfect gas. In this case we use the Gas constant coefficient for air.
- The air velocity inside and outside the incubator are low.
- The vapor condensation on the walls is neglected.
- The water boiler made by aluminium is a thermically thin body.
- There is mass conservation of dry air inside the incubator.
- Heat exchange through the glance is neglected.
- For an elementary volume in the enclosure, the air preserves its isothermal and isohydric properties.
- Soret and Dufour effects are neglected.

Taking into account these hypotheses, the various physical phenomena in the system are presented in Figure 2.

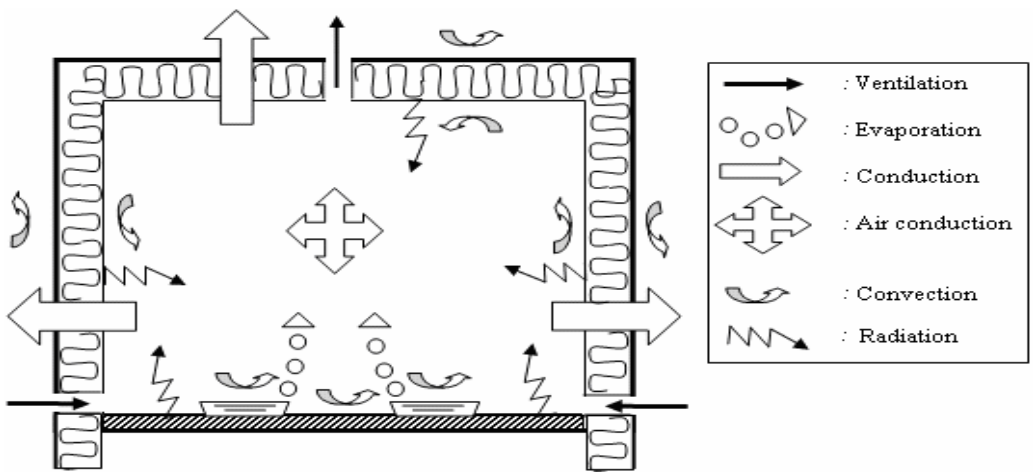

Figure 2: Mass and thermal transfers in the incubator

2. 3. Mass balance

Modelling is based mainly on the nodal method [3]. It consists of the subdivision the internal of the system into many zones. Each zone has presumably the same humidity and isothermal property. Thus, the enclosure was subdivided into 27 fictitious cells. Each cell has 3 equal dimensions along the axes (Oxyz) and elementary volume $\Delta v = \Delta x.\Delta y.\Delta z$ (Figure 3). The choice of the subdivision lies in the fact that the device has a symmetric position.

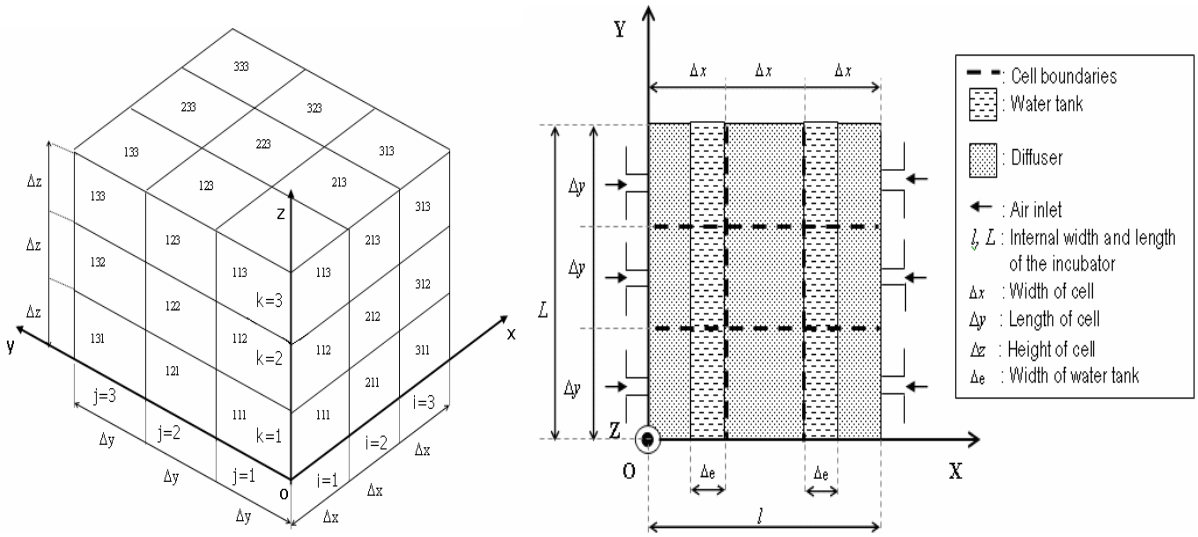

Figure 3. Cell division and distribution of devices (ventilating, humidifying and heating) inside the incubator.

Fick's law is used to define the vapor diffusion where the diffusion coefficient *Dc* is expressed by Shirmer's equation. The vapor released from the water tank into the cell depends on the water surface $\Delta x_e \Delta y$. According to the cell location, the total mass balance takes into account the mass transfer by the renewal of air through the inlet orifice, the evaporation from water tank, the air exchange at the outlet and the vapor diffusion between zones along the tree axes (Oxyz) and is given by [4, 5]:

$$\begin{aligned}\rho_{ijk}\frac{\Delta v}{\Delta t}(C_{ijk}-C^*_{ijk}) &= (1-\delta_i^2)\delta_k^1(\rho_e \overset{\circ}{V}_e C_e + 0{,}92\frac{h_v}{\rho_s Cp_s}\Delta x_e \Delta y(\frac{R_s}{V_s}-\frac{R_{ijk}}{V_{ijk}})) - \delta_i^2\delta_j^2\delta_k^3\rho_e n_t \overset{\circ}{V}_e(1-C_e)\frac{C_m}{1-C_m} \\ &+ (1-\delta_i^1)\rho_{ijk}\frac{Dc_{ijk}}{\Delta x}\left(\frac{C_{i-1jk}-C_{ijk}}{\Delta x}\right) + (1-\delta_i^3)\rho_{ijk}\frac{Dc_{ijk}}{\Delta x}\left(\frac{C_{i+1jk}-C_{ijk}}{\Delta x}\right) \\ &+ (1-\delta_j^1)\rho_{ijk}\frac{Dc_{ijk}}{\Delta y}\left(\frac{C_{ij-1k}-C_{ijk}}{\Delta y}\right) + (1-\delta_j^3)\rho_{ijk}\frac{Dc_{ijk}}{\Delta y}\left(\frac{C_{,j+1k}-C_{ijk}}{\Delta y}\right) \\ &+ (1-\delta_k^1)\rho_{ijk}\frac{Dc_{ijk}}{\Delta z}\left(\frac{C_{ijk-1}-C_{ijk}}{\Delta z}\right) + (1-\delta_k^3)\rho_{ijk\,1}\frac{Dc_{ijk}}{\Delta z}\left(\frac{C_{ijk+1}-C_{ijk}}{\Delta z}\right)\end{aligned} \quad (1)$$

The Kronecker symbol δ is used to specify each cell's position. V_e indicates the air flow rate through each air inlet, and $V_e\ n_t$ gives the total air flow rate. Taking into account the symmetry of the system, only 12 cells are left as shown in figure 4. Consequently, equation 1 can be reduced into 12 equations.

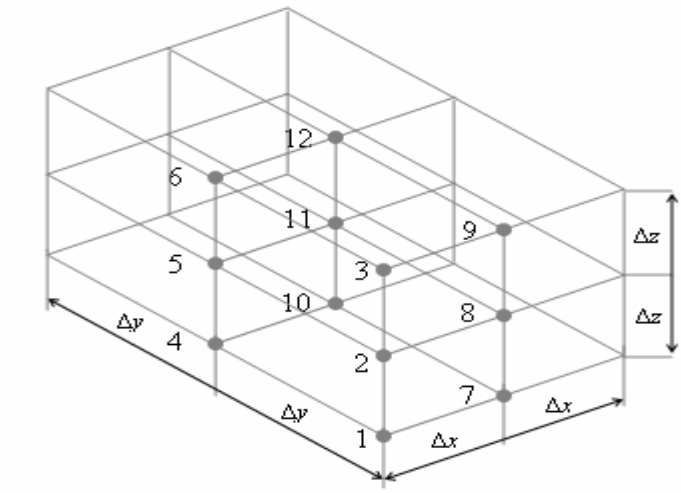

Figure 4: Diagram showing the cell nodes in the incubator

Therefore, the mass balance equation can be written in simple matrix form

$$A \times C = B \quad (2)$$

where,

$$
A=\begin{bmatrix}
\alpha_1 & \beta_1/\Delta z^2 & 0 & \beta_1/\Delta y^2 & 0 & 0 & \beta_1/\Delta x^2 & 0 & 0 & 0 & 0 & 0 \\
\beta_2/\Delta z^2 & \alpha_2 & \beta_2/\Delta z^2 & 0 & \beta_2/\Delta y^2 & 0 & 0 & \beta_2/\Delta x^2 & 0 & 0 & 0 & 0 \\
0 & \beta_3/\Delta z^2 & \alpha_3 & 0 & 0 & \beta_3/\Delta y^2 & 0 & 0 & \beta_3/\Delta x^2 & 0 & 0 & 0 \\
2\beta_4/\Delta y^2 & 0 & 0 & \alpha_4 & \beta_4/\Delta z^2 & 0 & 0 & 0 & 0 & \beta_4/\Delta x^2 & 0 & 0 \\
0 & 2\beta_5/\Delta y^2 & 0 & \beta_5/\Delta z^2 & \alpha_5 & \beta_5/\Delta z^2 & 0 & 0 & 0 & 0 & \beta_5/\Delta x^2 & 0 \\
0 & 0 & 2\beta_6/\Delta y^2 & 0 & \beta_6/\Delta z^2 & \alpha_6 & 0 & 0 & 0 & 0 & 0 & \beta_6/\Delta x^2 \\
2\beta_7/\Delta x^2 & 0 & 0 & 0 & 0 & 0 & \alpha_7 & \beta_7/\Delta z^2 & 0 & \beta_7/\Delta y^2 & 0 & 0 \\
0 & 2\beta_8/\Delta x^2 & 0 & 0 & 0 & 0 & \beta_8/\Delta z^2 & \alpha_8 & \beta_8/\Delta z^2 & 0 & \beta_8/\Delta y^2 & 0 \\
0 & 0 & 2\beta_9/\Delta x^2 & 0 & 0 & 0 & 0 & \beta_9/\Delta z^2 & \alpha_9 & 0 & 0 & \beta_9/\Delta y^2 \\
0 & 0 & 0 & 2\beta_{10}/\Delta x^2 & 0 & 0 & 2\beta_{10}/\Delta y^2 & 0 & 0 & \alpha_{10} & \beta_{10}/\Delta z^2 & 0 \\
0 & 0 & 0 & 0 & 2\beta_{11}/\Delta x^2 & 0 & 0 & 2\beta_{11}/\Delta y^2 & 0 & \beta_{11}/\Delta z^2 & \alpha_{11} & \beta_{11}/\Delta z^2 \\
0 & 0 & 0 & 0 & 0 & 2\beta_{12}/\Delta x^2 & 0 & 0 & 2\beta_{12}/\Delta y^2 & 0 & \beta_{12}/\Delta z^2 & \alpha_{12}
\end{bmatrix} \quad (3)
$$

For *i=1..12*, the matrix elements are:

$$
\left.\begin{aligned}
\beta_i &= \rho_i.Dc_i.\Delta v \\
\alpha_i &= -\frac{\rho_i.\Delta v}{\Delta t} + \sum_{j=1,\, j\neq i}^{12} A_{ij}
\end{aligned}\right\} \quad (4)
$$

For the B vector:

$$
B=-\begin{pmatrix}
\frac{\rho_1.\Delta v}{\Delta t}.C_1^* + \rho_e.\overset{o}{V}_e.Ce + 0{,}92\frac{h_v}{\rho_s Cp_s}\Delta x_e \Delta y(\frac{R_s}{V_s}-\frac{R_1}{V_1}) \\
\frac{\rho_2.\Delta v}{\Delta t}.C_2^* \\
\frac{\rho_3.\Delta v}{\Delta t}.C_3^* \\
\frac{\rho_4.\Delta v}{\Delta t}.C_4^* + \rho_e.\overset{o}{V}_e.Ce + 0{,}92\frac{h_v}{\rho_s Cp_s}\Delta x_e \Delta y(\frac{R_s}{V_s}-\frac{R_4}{V_4}) \\
\frac{\rho_5.\Delta v}{\Delta t}.C_5^* \\
\frac{\rho_6.\Delta v}{\Delta t}.C_6^* \\
\frac{\rho_7.\Delta v}{\Delta t}.C_7^* \\
\frac{\rho_8.\Delta v}{\Delta t}.C_8^* \\
\frac{\rho_9.\Delta v}{\Delta t}.C_9^* \\
\frac{\rho_{10}.\Delta v}{\Delta t}.C_{10}^* \\
\frac{\rho_{11}.\Delta v}{\Delta t}.C_{11}^* \\
\frac{\rho_{12}.\Delta v}{\Delta t}.C_{12}^* + n_t.\overset{o}{V}_e.(1-Ce))\frac{C_m}{1-C_m}
\end{pmatrix} \quad (5)
$$

2. 4. Heat balance

Heat balance between the cells required internal wall temperature value. For example, the external and internal wall temperatures in plan (Oxz) can be determined in the following equations:

$$\left.\begin{aligned}
\rho_b S_b e_b Cp_b \frac{(T_{pe_{ijk}} - T^*_{pe_{ijk}})}{\Delta t} &= h_{ve} S_b (T_e - T_{pe_{ijk}}) + h_{eqb} S_b (T_{px_{ijk}} - T_{pex_{ijk}}) \\
\rho_b S_b e_b Cp_b \frac{(T_{px_{ijk}} - T^*_{px_{ijk}})}{\Delta t} &= h_{eqb} S_b (T_{pex_{ijk}} - T_{px_{ijk}}) + h_{eqx_{ijk}} S_b (T_{ijk} - T_{px_{ijk}}) + \textstyle\sum_{q=1}^{5} h_{r_q} F_{xq} S_b (T_{pm_q} - T_{px_{ijk}})
\end{aligned}\right\} \quad (6)$$

These equations use the global heat transfer coefficient for thermal conductivity and thermal convection for each node. Every internal wall of the cells is in heat radiation with 5 walls (*p=1..5*). The form factor is deduced from the Nusselt's analog by mainly using the hemisphere method.

After knowing the wall temperature's value, the thermal balance for all cells [5, 6, 7] is written as:

$$\begin{aligned}
\rho_{ijk} Cp_{ijk} \frac{\Delta v}{\Delta t}(T_{ijk} - T^*_{ijk}) &= (1-\delta_i^2)\delta_k^1 \rho_e \overset{\circ}{V}_e Cp_e (T_e - T_{ijk}) + 0{,}92 \frac{h_{vd}}{\rho_s Cp_s} \Delta e \Delta y \left(\frac{R_s}{V_s} - \frac{R_{ijk}}{V_{ijk}}\right) Cp_v (T_d - T_{ijk}) \\
&- \delta_i^2 \delta_j^2 \delta_k^3 \rho_e \overset{\circ}{V}_e (1-C_e) Cp_e \frac{1}{1-C_m}(T_e - T_{ijk}) + (1-\delta_1^2) h_{eqx_{ijk}} \frac{\Delta v}{\Delta x}(T_{px_{ijk}} - T_{ijk}) \\
&+ (1-\delta_j^2) h_{eqy_{ijk}} \frac{\Delta v}{\Delta y}(T_{py_{ijk}} - T_{ijk}) + \delta_k^3 h_{eqz_{ijk}} \frac{\Delta v}{\Delta z}(T_{pz_{izk}} - T_{ijk}) + \delta_k^1 h_{eqd_{ijk}} \frac{\Delta v}{\Delta z}(T_d - T_{ijk}) \\
&+ (1-\delta_i^1)\lambda_{ijk} \frac{\Delta v}{\Delta x^2}(T_{i-1jk} - T_{ijk}) + (1-\delta_i^3)\lambda_{ijk} \frac{\Delta v}{\Delta x^2}(T_{i+1jk} - T_{ijk}) \\
&+ (1-\delta_j^1)\lambda_{ijk} \frac{\Delta v}{\Delta y^2}(T_{ij-1k} - T_{ijk}) + (1-\delta_j^3)\lambda_{ijk} \frac{\Delta v}{\Delta y^2}(T_{ij+1k} - T_{ijk}) \\
&+ (1-\delta_k^1)\lambda_{ijk} \frac{\Delta v}{\Delta z^2}(T_{ijk-1} - T_{ijk}) + (1-\delta_k^3)\lambda_{ijk} \frac{\Delta v}{\Delta z^2}(T_{ijk+1} - T_{ijk})
\end{aligned} \quad (7)$$

Using the same transformations as used in the mass balance, the equation (7) can be written to matrix form:

$$D \times T = E \quad (8)$$

Where,

$$D = \begin{bmatrix}
\alpha_1 & \beta_1/\Delta z^2 & 0 & \beta_1/\Delta y^2 & 0 & 0 & \beta_1/\Delta x^2 & 0 & 0 & 0 & 0 & 0 \\
\beta_2/\Delta z^2 & \alpha_2 & \beta_2/\Delta z^2 & 0 & \beta_2/\Delta y^2 & 0 & 0 & \beta_2/\Delta x^2 & 0 & 0 & 0 & 0 \\
0 & \beta_3/\Delta z^2 & \alpha_3 & 0 & 0 & \beta_3/\Delta y^2 & 0 & 0 & \beta_3/\Delta x^2 & 0 & 0 & 0 \\
2\beta_4/\Delta y^2 & 0 & 0 & \alpha_4 & \beta_4/\Delta z^2 & 0 & 0 & 0 & 0 & \beta_4/\Delta x^2 & 0 & 0 \\
0 & 2\beta_5/\Delta y^2 & 0 & \beta_5/\Delta z^2 & \alpha_5 & \beta_5/\Delta z^2 & 0 & 0 & 0 & 0 & \beta_5/\Delta x^2 & 0 \\
0 & 0 & 2\beta_6/\Delta y^2 & 0 & \beta_6/\Delta z^2 & \alpha_6 & 0 & 0 & 0 & 0 & 0 & \beta_6/\Delta x^2 \\
2\beta_7/\Delta x^2 & 0 & 0 & 0 & 0 & 0 & \alpha_7 & \beta_7/\Delta z^2 & 0 & \beta_7/\Delta y^2 & 0 & 0 \\
0 & 2\beta_8/\Delta x^2 & 0 & 0 & 0 & 0 & \beta_7/\Delta z^2 & \alpha_8 & \beta_8/\Delta z^2 & 0 & \beta_8/\Delta y^2 & 0 \\
0 & 0 & 2\beta_9/\Delta x^2 & 0 & 0 & 0 & 0 & \beta_8/\Delta z^2 & \alpha_9 & 0 & 0 & \beta_9/\Delta y^2 \\
0 & 0 & 0 & 2\beta_{10}/\Delta x^2 & 0 & 0 & 2\beta_{10}/\Delta y^2 & 0 & 0 & \alpha_{10} & \beta_{10}/\Delta z^2 & 0 \\
0 & 0 & 0 & 0 & 2\beta_{11}/\Delta x^2 & 0 & 0 & 2\beta_{11}/\Delta y^2 & 0 & \beta_{11}/\Delta z^2 & \alpha_{11} & \beta_{11}/\Delta z^2 \\
0 & 0 & 0 & 0 & 0 & 2\beta_{12}/\Delta x^2 & 0 & 0 & 2\beta_{12}/\Delta y^2 & 0 & \beta_{12}/\Delta z^2 & \alpha_{12}
\end{bmatrix} \quad (9)$$

The above matrix *D* shows the heat exchange between the cells and is similar to matrix A (3) in which

$$\beta_i = \lambda_i \ (i=1..12), \quad (10)$$

and diagonal elements α_i are derived from α vector such as:

$$
\alpha = -\begin{pmatrix}
\frac{\rho_1 Cp_1 \Delta v}{\Delta t} + \sum_{j=1, j\neq 1}^{12} M_{1j} + h_{eq\,x_1}\frac{\Delta v}{\Delta x} + h_{eq\,y_1}\frac{\Delta v}{\Delta y} + h_{eq\,d_1}\frac{\Delta v}{\Delta z} + \rho_e \overset{\circ}{V}_e Cp_e + 0{,}92\frac{h_{vd}}{\rho_s Cp_s}\Delta x_e \Delta y\left(\frac{R_3}{V_3} - \frac{R_1}{V_1}\right)Cp_v \\
\frac{\rho_2 Cp_2 \Delta v}{\Delta t} + \sum_{j=1, j\neq 2}^{12} M_{2j} + h_{eq\,x_2}\frac{\Delta v}{\Delta x} + h_{eq\,y_2}\frac{\Delta v}{\Delta y} \\
\frac{\rho_3 Cp_3 \Delta v}{\Delta t} + \sum_{j=1, j\neq 3}^{12} M_{3j} + h_{eq\,x_3}\frac{\Delta v}{\Delta x} + h_{eq\,y_3}\frac{\Delta v}{\Delta y} + h_{eq\,z_3}\frac{\Delta v}{\Delta z} \\
\frac{\rho_4 Cp_4 \Delta v}{\Delta t} + \sum_{j=1, j\neq 4}^{12} M_{4j} + h_{eq\,y_4}\frac{\Delta v}{\Delta y} + h_{eq\,d_4}\frac{\Delta v}{\Delta z} + \rho_e \overset{\circ}{V}_e Cp_e + 0{,}92\frac{h_{vd}}{\rho_s Cp_s}\Delta e \Delta y\left(\frac{R_3}{V_3} - \frac{R_4}{V_4}\right)Cp_v \\
\frac{\rho_5 Cp_5 \Delta v}{\Delta t} + \sum_{j=1, j\neq 5}^{12} M_{5j} + h_{eq\,y_5}\frac{\Delta v}{\Delta y} \\
\frac{\rho_6 Cp_6 \Delta v}{\Delta t} + \sum_{j=1, j\neq 6}^{12} M_{6j} + h_{eq\,y_6}\frac{\Delta v}{\Delta y} + h_{eq\,z_6}\frac{\Delta v}{\Delta z} \\
\frac{\rho_7 Cp_7 \Delta v}{\Delta t} + \sum_{j=1, j\neq 7}^{12} M_{7j} + h_{eq\,x_7}\frac{\Delta v}{\Delta x} + h_{eq\,d_7}\frac{\Delta v}{\Delta z} \\
\frac{\rho_8 Cp_8 \Delta v}{\Delta t} + \sum_{j=1, j\neq 8}^{12} M_{8j} + h_{eq\,x_8}\frac{\Delta v}{\Delta x} \\
\frac{\rho_9 Cp_9 \Delta v}{\Delta t} + \sum_{j=1, j\neq 9}^{12} M_{9j} + h_{eq\,x_9}\frac{\Delta v}{\Delta x} + h_{eq\,z_9}\frac{\Delta v}{\Delta z} \\
\frac{\rho_{10} Cp_{10} \Delta v}{\Delta t} + \sum_{j=1, j\neq 10}^{12} M_{10j} + h_{eq\,d_{10}}\frac{\Delta v}{\Delta z} \\
\frac{\rho_{11} Cp_{11} \Delta v}{\Delta t} + \sum_{j=1, j\neq 11}^{12} M_{11j} \\
\frac{\rho_{12} Cp_{12} \Delta v}{\Delta t} + \sum_{j=1, j\neq 12}^{12} M_{12j} + h_{eq\,z_{12}}\frac{\Delta v}{\Delta z} - \rho_e \eta_i \overset{\circ}{V}_e (1 - C_e))Cp_e \frac{1}{1 - C_m}
\end{pmatrix} \quad (11)
$$

For determining vector E its components are used to express E_i

$$
E = -\begin{pmatrix}
\frac{\rho_1 Cp_1 \Delta v}{\Delta t} T_1^* + h_{eq\,1}\frac{\Delta v}{\Delta x} T_{\rho\,1} + h_{eq\,1}\frac{\Delta v}{\Delta y} Tp_{y_1} + h_{eq\,d_1}\frac{\Delta v}{\Delta z} T_d + \rho_e \overset{\circ}{V}_1 Cp_e T_e + 0{,}92\frac{h_{vd}}{\rho_s Cp_s}\Delta e \Delta y\left(\frac{R_3}{V_3} - \frac{R_1}{V_1}\right)Cp_v T_d \\
\frac{\rho_2 Cp_2 \Delta v}{\Delta t} T_2^* + h_{eq\,x_2}\frac{\Delta v}{\Delta x} T_{\rho\,x_2} + h_{eq\,y_2}\frac{\Delta v}{\Delta y} T_{\rho\,y_2} \\
\frac{\rho_3 Cp_3 \Delta v}{\Delta t} T_3^* + h_{eq\,x_3}\frac{\Delta v}{\Delta x} T_{\rho\,x_3} + h_{eq\,y_3}\frac{\Delta v}{\Delta y} T_{\rho\,y_3} + h_{eq\,z_3}\frac{\Delta v}{\Delta z} Tp_{z_3} \\
\frac{\rho_4 Cp_4 \Delta v}{\Delta t} T_4^* + h_{eq\,x_4}\frac{\Delta v}{\Delta y} T_{\rho\,y_4} + h_{eq\,d_4}\frac{\Delta v}{\Delta z} T_d + \rho_e \overset{\circ}{V}_e Cp_e T_e + 0{,}92\frac{h_{vd}}{\rho_s Cp_s}\Delta e \Delta y\left(\frac{R_3}{V_3} - \frac{R_4}{V_4}\right)Cp_v T_d \\
\frac{\rho_5 Cp_5 \Delta v}{\Delta t} T_5^* + h_{eq\,y_5}\frac{\Delta v}{\Delta y} T_{\rho\,y_5} \\
\frac{\rho_6 Cp_6 \Delta v}{\Delta t} T_6^* + h_{eq\,y_6}\frac{\Delta v}{\Delta y} T_{\rho\,y_6} + h_{eq\,z_6}\frac{\Delta v}{\Delta z} T_{\rho\,z_6} \\
\frac{\rho_7 Cp_7 \Delta v}{\Delta t} T_7^* + h_{eq\,x_7}\frac{\Delta v}{\Delta x} T_{\rho\,x_7} + h_{eq\,d_7}\frac{\Delta v}{\Delta z} T_d \\
\frac{\rho_8 Cp_8 \Delta v}{\Delta t} T_8^* + h_{eq\,x_8}\frac{\Delta v}{\Delta x} T_{\rho\,x_8} \\
\frac{\rho_9 Cp_9 \Delta v}{\Delta t} T_9^* + h_{eq\,x_9}\frac{\Delta v}{\Delta x} T_{\rho\,x_9} + h_{eq\,z_9}\frac{\Delta v}{\Delta z} T_{\rho\,z_9} \\
\frac{\rho_{10} Cp_{10} \Delta v}{\Delta t} T_{10}^* + h_{eq\,d_{10}}\frac{\Delta v}{\Delta z} T_d \\
\frac{\rho_{11} Cp_{11} \Delta v}{\Delta t} T_{11}^* \\
\frac{\rho_{12} Cp_{12} \Delta v}{\Delta t} T_{12}^* + h_{eq\,z_{12}}\frac{\Delta v}{\Delta z} T_{\rho\,z_{12}} - \rho_e \eta_i \overset{\circ}{V}_e (1 - C_e) Cp_e \frac{1}{1 - C_m} T_e
\end{pmatrix} \quad (12)
$$

3. RESULTS AND DISCUSSION

The external temperature is 20°C and the relative humidity of the air 50%. The simulation were carried out by fixing in the model the temperature of the floor at 40°, the width of water tank is 5cm and the area of each opening is 1cm². Figures 4 and 5 represent vapor concentration and temperature distributions of simulation during preheat time.

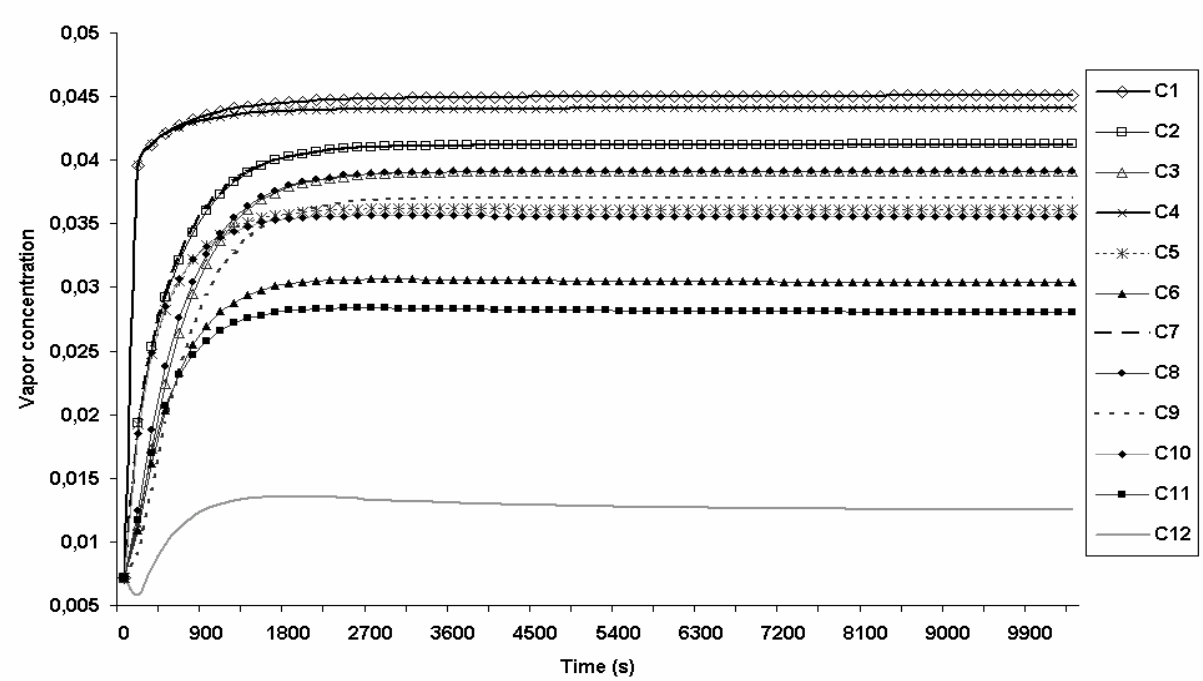

Figure 4: vapor concentration distribution in the 12 cells obtained by the model

The vapor concentration is high for cells 1 and 4 since both contain a water tank. Cell 12 is the least humid. During preheat time, the vapor concentration in cell 12 decreases for a while and then increases gradually till it reaches the steady state. In fact, the heat released by the heat diffuser introduces a huge concentration of dry air in this cell at the beginning. Then the vapor coming from water tank spreads up for a short time and fills cell 12. In cells 2, 5, 8 and 11 where the hatching plate is located, the vapor distribution is different. Indeed, cell 11 is the least humid. Cells 1 and 4 are very humid due to the fact that each of them contain a water tank. Generally, the results show vapor concentration stratifications in all of the cells.

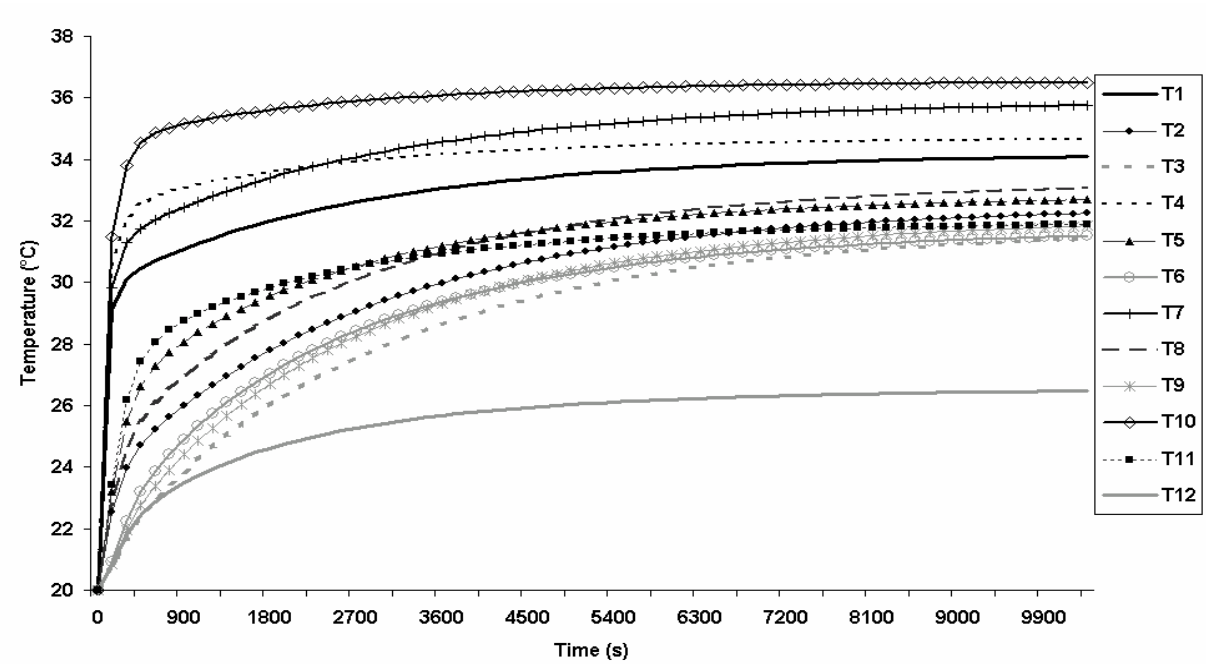

Figure 5: temperature distribution in the 12 cells obtained by the model.

As concerns the temperatures simulated by the model, cells 7 and 10 are the warmest. This is due to the fact that these two cells are in direct contact with the diffuser. Cells 1 and 4 are also situated above the diffuser; however their temperature is lower than cells 7 and 10. This is because they both contain a water tank and an air opening which reduces their temperature. Cell 12 is most cold and the rest of the cells vary according to their location. Generally, during preheat time the simulated temperatures are continuously increased and show a stratification until the steady state is reached. Also we deduced that isothermal surface is

not horizontal. At the hatching plate level, the model shows that cell 11 has the lowest temperature. At this level, the temperature variation is nearly 1°C.

In order to validate the model, the temperatures given by the simulation were compared to those measured in the experimentation. Table 2 shows the comparison of the temperatures at steady states for every cell and their absolute error.

Table 2. Comparison of the temperatures at steady states of the model and the experimental measure of the 12 cells and their absolute error.

N° cells	Temperature in steady states (°C)		Absolute error (°C)
	Model	Experimental measure	
1	34.09	34,00	0.09
2	32.25	35,00	2.75
3	31.43	32.25	0.82
4	34.66	34.16	0.5
5	32.69	34.40	1.71
6	31.51	33.25	1.74
7	35.75	35,00	0.75
8	33.06	34.20	1.14
9	31.83	34,00	2.17
10	36.51	38.12	1.61
11	31.89	35,00	3.11
12	26.47	34,00	7.53
Average	**32.76**	**34.15**	**1.37**

The experiment shows the temperature stratifications in all of the cells. The absolute error between the temperatures is even higher in cell 12 because in the analysis of the model it wasn't expected that the airflow at the outlet would be very high. Given that the cell's location is symmetric (figure 3), the average temperature of the model and experimental measure results are 32.76 and 34.15°C respectively. The simulation results are slightly lower than the experimentation ones. The average temperature results in the experimental measure and simulation are almost close to 1.37°C.

It is difficult to specify in the experiment when the temperature of the heat diffuser reaches exactly 40°C for measurement. The model shows that theoretically the heating takes around 174min for the configuration where all the openings of the ventilation are open. The preheat time for moisturising is reached faster than the one for temperature.

4. CONCLUSION

In this paper, the study shows that the conception of the model for the incubator requires a knowledge of the mass and heat transfer and the method of writing the equations. Despite the number of cells, the mass and heat balances can be written in one expression respectively using the Kronecker symbol. Writing the balance equations into matrix form facilitates programming and the resolution of the model.

As the isothermal and isohydric surfaces are not horizontal in parallel with the hatching plate, it is important to move the eggs especially when the orifices are open. When the orifices are closed, the temperature and vapor concentration variations at the hatching plate level decrease and their average values increase. To predict them, the opening area needs to be changed in the model. In conclusion, the model can determine the vapor concentration distribution in the incubator. Moreover it can be used to optimize the system functioning by indicating precisely the hatching plate location. In addition, the model has also the advantage of predicting the environment in the system which is related to other parameters like the width of water tank, the orifice, the diffuser temperature and the volume of the enclosure. By knowing the data characterizing the ideal environment for the incubation of a species, these parameters can be defined with precision by the model using sensitivity analysis.

5. REFERENCES

[1] Wageiningen, L'incubation des œufs par les poules ou en couveuse, Agromisa 1990.

[2] R. E. Yatter, Electric incubator for gamebird eggs, Journal of Wild life Management. vol. 10, n°4 (October 1946), pp. 342-347.

[3] J.B.Saulnier, A. Alexandre, La modélisation thermique par la méthode nodale: Ses principes, ses succès et ses limites, Rev. Gén. Therm, Fr, 280 (1985), pp. 363-372.

[4] B. Sauver, Reproduction des volailles et production des œufs, INRA Paris 1998.

[5] Dumargue, Ecoulements polyphasique en milieux poreux, 1983.

[6] Règles Th-77, Document technique unifié: Règles de calcul des caractéristiques utiles des parois de construction, Novembre 1977.

[7] M. Daguenet, Les séchoirs solaires : théorie et pratique, 1985.